Abundance of *Pelagia noctiluca* early life stages in the western Mediterranean Sea scales with surface chlorophyll

Daniel Ottmann*, Diego Álvarez-Berastegui, Laura Prieto, Rosa Balbín, Francisco Alemany, Øyvind Fiksen, Ana Gordoa, Patricia Reglero

*Corresponding author: daniel.ottmann.riera@gmail.com

S1. Supplementary methods:

To relate the vertical distribution of *Pelagia noctiluca* early life stages to the 0-100 m depth profiles of water temperature and fluorescence, we towed a Multinet Midi (0.25-m^2 opening mouth) at 2 knots speed and deployed a CTD roseate immediately afterwards. Given that the Multinet has 5 opening-and-closing nets, we sampled five 20-m strata from 100 m depth to surface. To ensure that our samples were representative, we increased the sampling effort targeting to filter at least 100 m^3 of water per net. Therefore, after deploying the Multinet down to 130 m at a winch speed of 40 m $minut^{-1}$ (Fig. S1a) and letting it stabilize for 5 minutes (Fig. S1b), we hauled the instrument at a winch speed of 2 m $minut^{-1}$ (Fig. S1c). The nets opened and closed automatically starting at 100 m depth following pressure thresholds and filtered 200 m^3 on average. Given that each operation toke almost 1.5 hours, we prevented the boat moving too far away from our initial location by navigating in circles of about 900 m in diameter. At the end of each Multinet operation a CTD rosette was deployed in the midpoint of the circumference (Fig. S1d).

Figure S1. Sampling design with Multinet midi to determine the vertical distribution of *P. noctiluca* early life stages in the first 100 m.

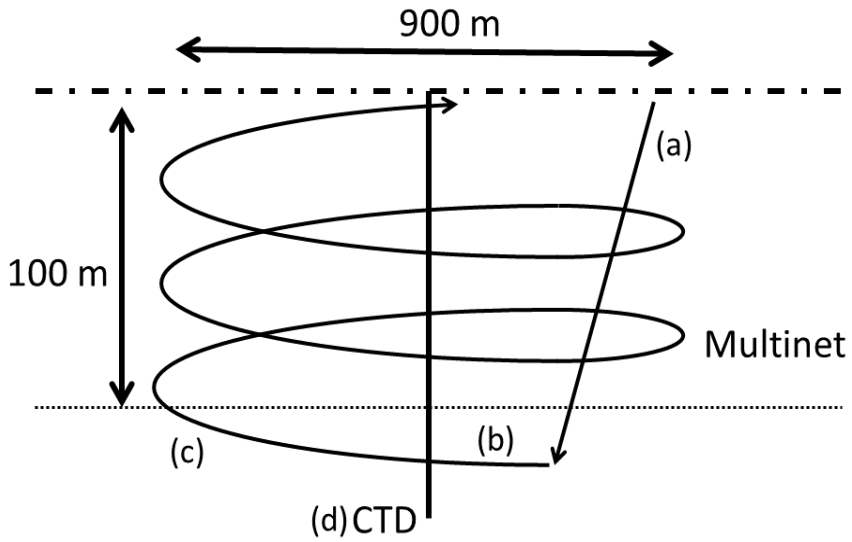

S2. Sensitivity analysis:

Table S1 Sensitivity analysis of the effect of monthly-mean surface chlorophyll a concentration of the study area on the interannual variability in abundance of *Pelagia noctiluca* early life stages. Annual mean densities were regressed against the monthly-mean chlorophyll concentration of June-July. The last column shows the monthly mean chlorophyll-a concentration averaged across all 6 study years, showing that chlorophyll peak in February and decreased throughout the following months. Chlorophyll *a* data was obtained from the Mediterranean Sea biogeochemistry reanalysis product v2.2 of the E.U. Copernicus Marine Servei Information.

Month	p-value	Adjusted R^2	Monthly mean Chl-a concentration (6-year average)
January	0.471	0.47	0.256
February	0.625	0.62	0.286
March	0.058	0.54	0.211
April	**0.036***	**0.64**	**0.094**
May	**0.046***	**0.59**	**0.062**
June	**0.002****	**0.91**	**0.051**
July	0.439	-0.05	0.047

S3. Statistical model diagnostic plots:

Figure S2. Model diagnostics of binomial **model M2** after model selection. a) Recover operating characteristic (ROC) curve showing an area under the curve (AUC) of 94.4%; b) Probability of the model to predict true presences and true absences.

a)

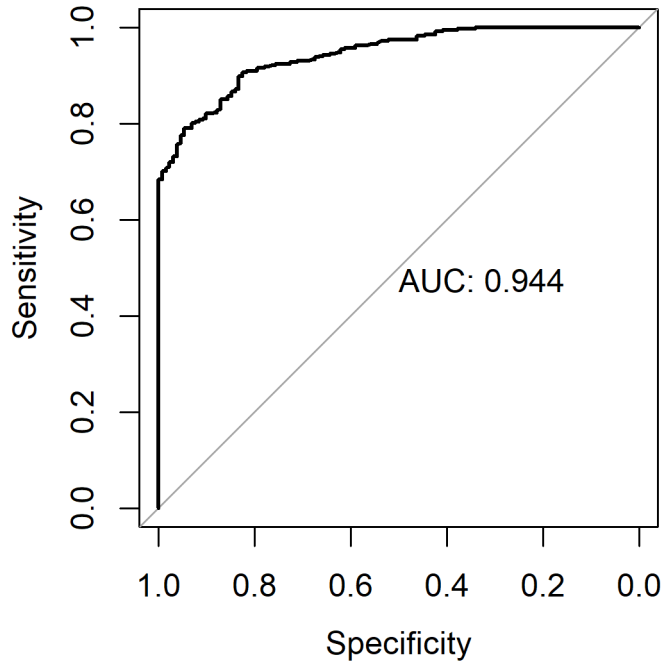

b)

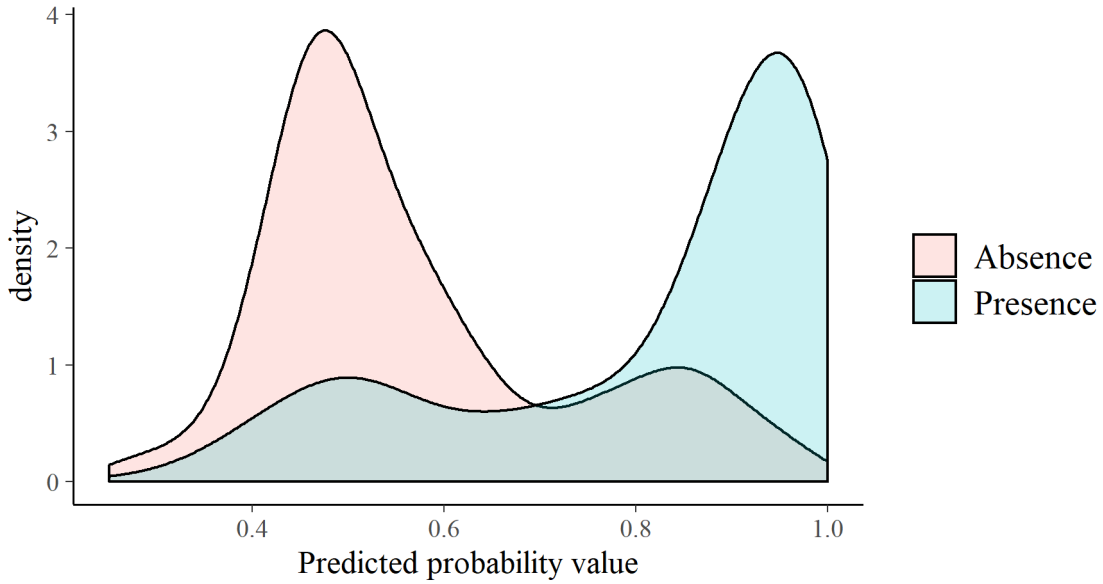

Figure S3. Mixing of Markov chain Monte Carlo (MCMC) chains (right) and the respective density plot (left) of the Bayesian **model M3** variables after model selection. Chains were thinned at 1/10. a) Random effect of year; b) Smoothing term for calendar day; c) Smoothing term for time of the day; d) Smoothing term for surface chlorophyll concentration.

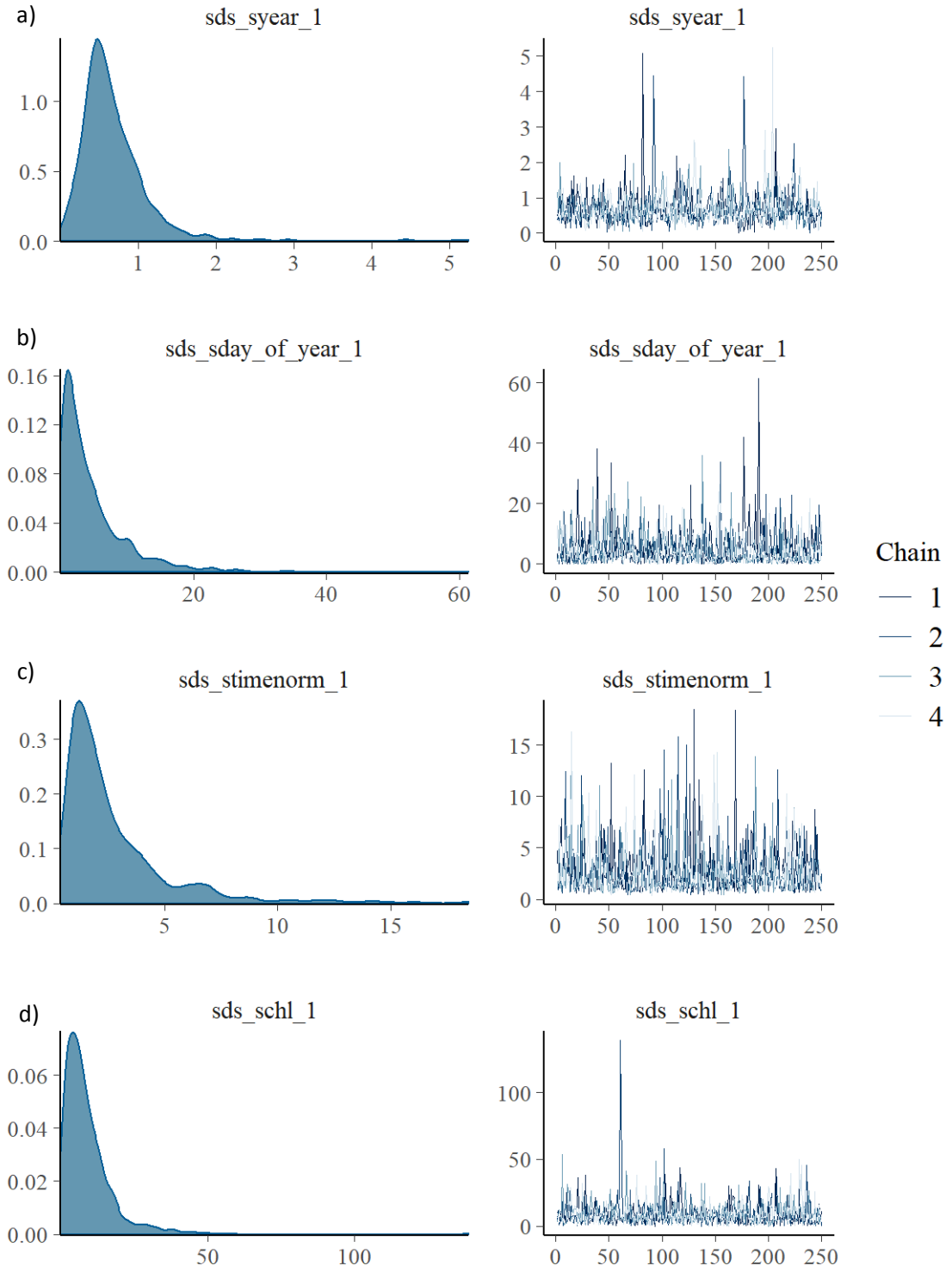

Figure S4. Model diagnostics of the selected **model M3**. a) Frequency distribution of *P. noctiluca* individuals collected in bongo tows in 2012-17 (dark blue) compared to distributions drawn from 100 posterior samples of the model (light blue). X-axis is truncated at 2000 *P. noctiluca* tow^{-1} to facilitate visualization; b) Pareto smoothed importance sampling (PSIS) diagnostic plot showing 99.8% of the values below 0.7; c) Leave one out-probability integral transformation (LOO-PIT) values compared to standard uniform distribution.

a)

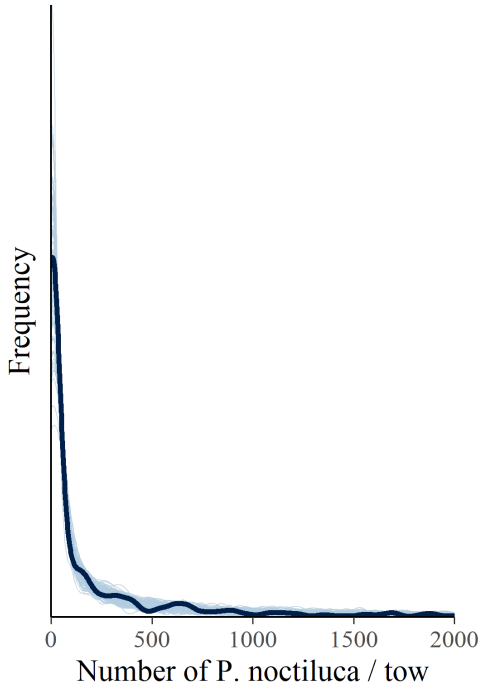

b)

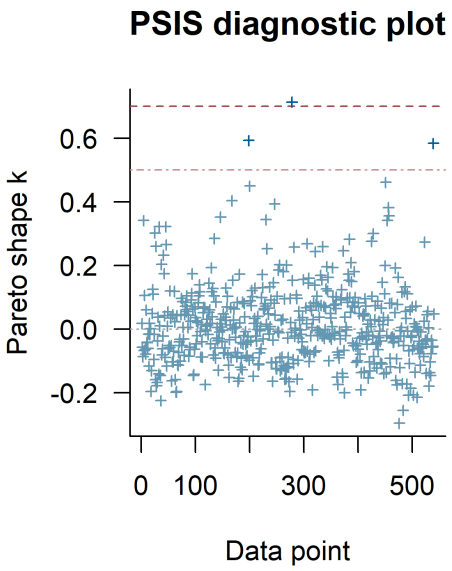

c)

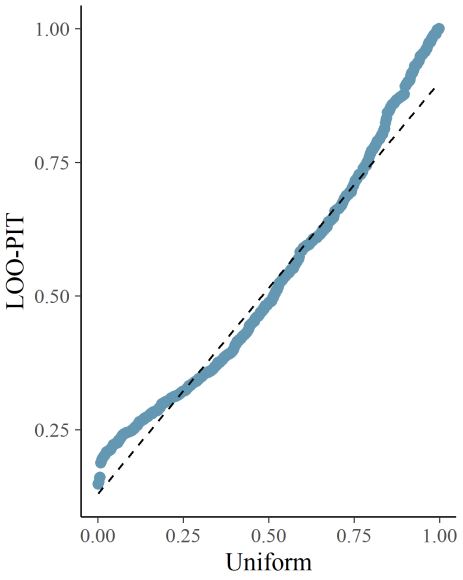

Figure S5. Model diagnostics of binomial **model M4** after model selection. a) Recover operating characteristic (ROC) curve showing an area under the curve (AUC) of 82.5%; b) Probability of the model to predict true presences and true absences.

a)

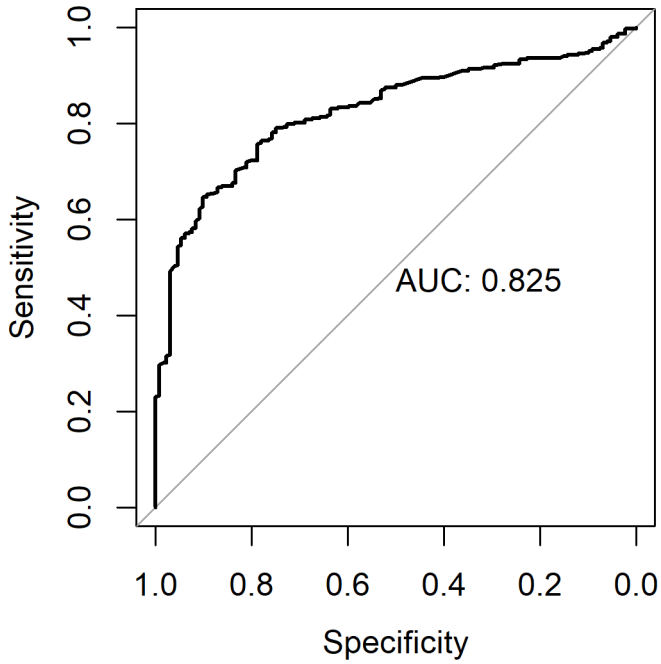

b)

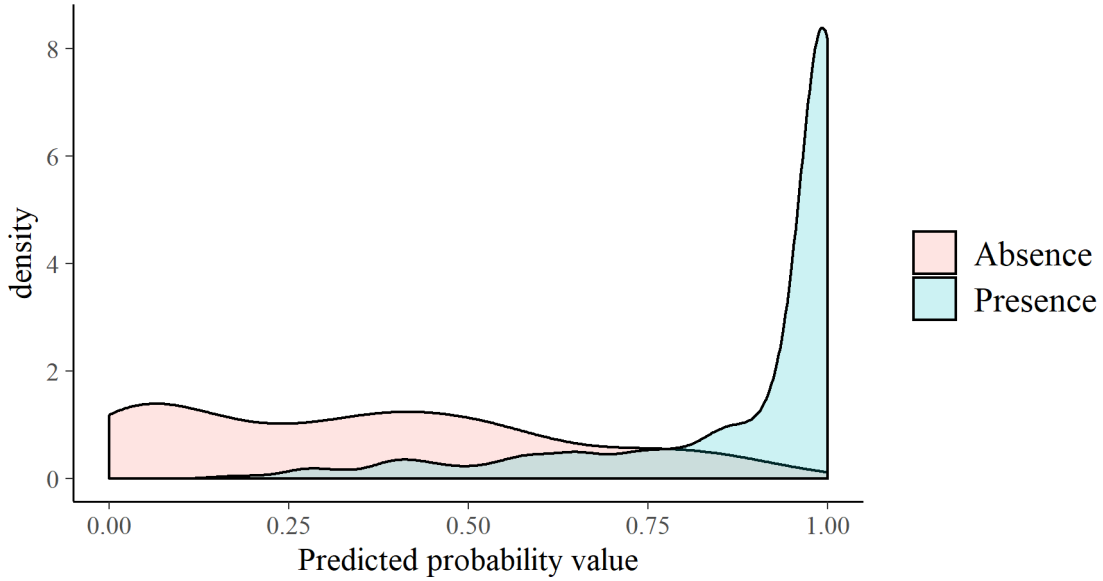

Figure S6. Mixing of Markov chain Monte Carlo (MCMC) chains (right) and the respective density plot (left) of the Bayesian **model M5** variables after model selection. Chains were thinned at 1/10. a) Smoothing term for latitude-longitude; b) Random effect of year; c) Smoothing term for calendar day; d) Smoothing term for time of the day; e) Smoothing term for surface chlorophyll concentration.

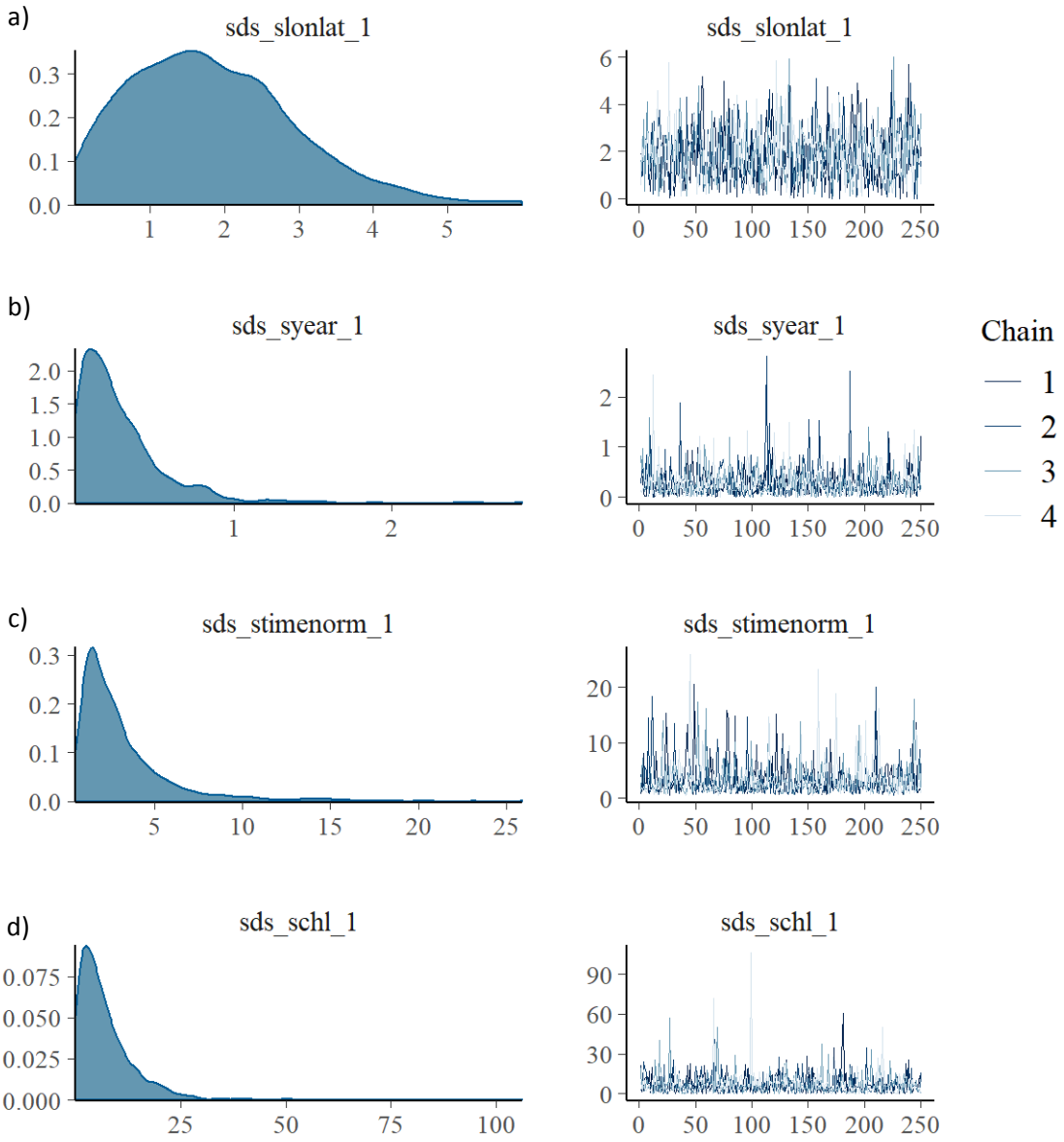

Figure S7. Model diagnostics of the selected **model M5**. a) Frequency distribution of *Pelagia noctiluca* individuals collected in bongo tows in 2012-17 (dark blue) compared to distributions drawn from 100 posterior samples of the model (light blue). X-axis is truncated at 2000 *P. noctiluca* tow^{-1} to facilitate visualization; b) Pareto smoothed importance sampling (PSIS) diagnostic plot showing 99.3% of the values below 0.7; c) Leave one out-probability integral transformation (LOO-PIT) values compared to standard uniform distribution.

a)

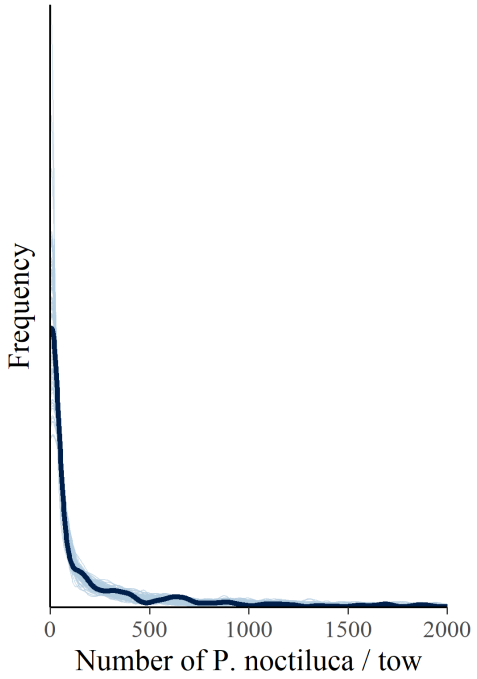

b)

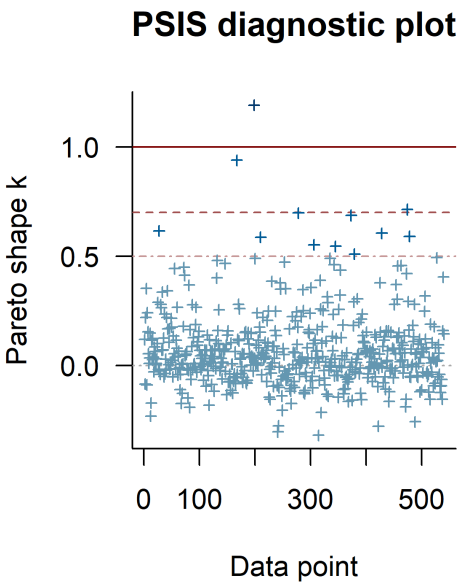

c)

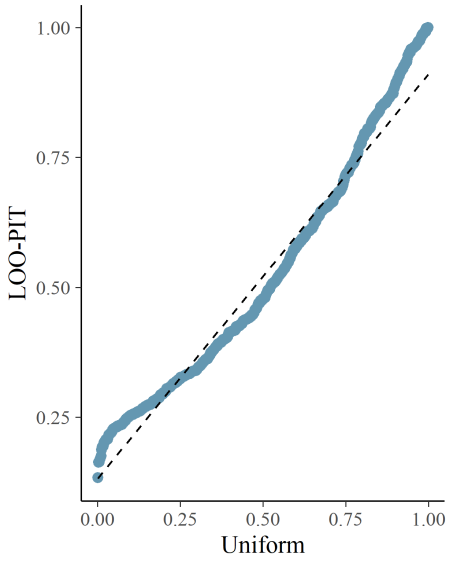

Figure S8. Model diagnostics of **model M6** after model selection. This model uses n = 6 annual average values of *P. noctiluca* densities and surface chlorophyll concentration. a) Residuals vs. fitted values; b) Quantile-quantile plot.

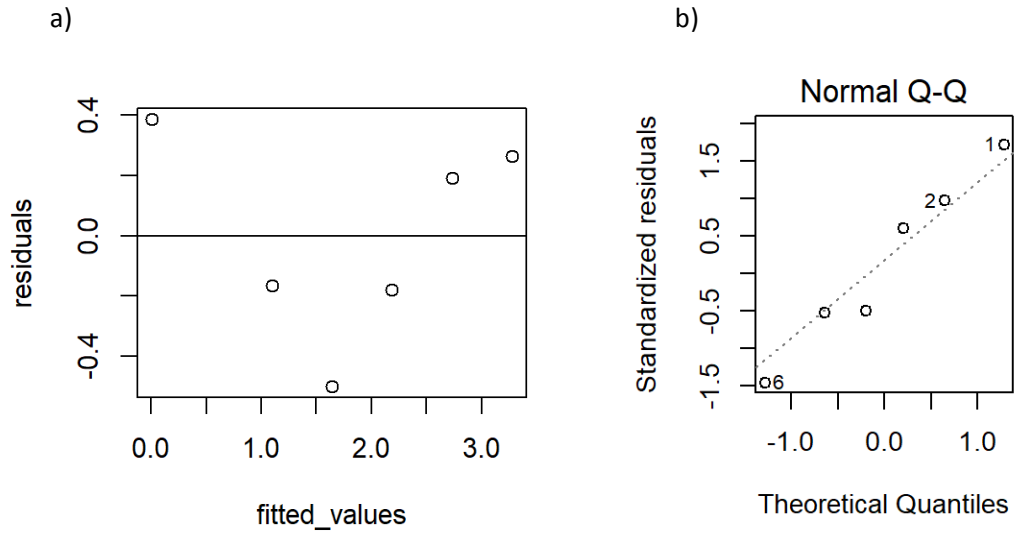

Figure S9. Mixing of Markov chain Monte Carlo (MCMC) chains (right) and the respective density plot (left) of the Bayesian **model M7** variables after model selection. Chains were thinned at 1/10. a) Smoothing term for calendar day; b) Smoothing term for time of the day; c) Smoothing term for mean surface chlorophyll concentration of the study area.